Annals of Botany **119**: 191–205, 2017
doi:10.1093/aob/mcw226, available online at www.aob.oxfordjournals.org

ANNALS OF BOTANY
Founded 1887

Photosynthetic induction and its diffusional, carboxylation and electron transport processes as affected by CO_2 partial pressure, temperature, air humidity and blue irradiance

Elias Kaiser[1,*], Johannes Kromdijk[2], Jeremy Harbinson[1], Ep Heuvelink[1] and Leo F. M. Marcelis[1]

[1]Horticulture and Product Physiology Group, Wageningen University, Droevendaalsesteeg 1, 6708 PB Wageningen, the Netherlands and [2]Institute for Genomic Biology, University of Illinois, 1206 West Gregory Drive, Urbana, IL, USA
**For correspondence. Present address: Wageningen UR Greenhouse Horticulture, Droevendaalsesteeg 1, 6708 PB Wageningen, the Netherlands. E-mail elias.kaiser@wur.nl*

Received: 31 May 2016 Returned for revision: 8 July 2016 Editorial decision: 14 September 2016 Published electronically: 26 December 2016

• **Background and Aims** Plants depend on photosynthesis for growth. In nature, factors such as temperature, humidity, CO_2 partial pressure, and spectrum and intensity of irradiance often fluctuate. Whereas irradiance intensity is most influential and has been studied in detail, understanding of interactions with other factors is lacking.
• **Methods** We tested how photosynthetic induction after dark–light transitions was affected by CO_2 partial pressure (20, 40, 80 Pa), leaf temperatures (15·5, 22·8, 30·5 °C), leaf-to-air vapour pressure deficits ($VPD_{leaf\text{-}air}$; 0·5, 0·8, 1·6, 2·3 kPa) and blue irradiance (0–20 %) in tomato leaves (*Solanum lycopersicum*).
• **Key Results** Rates of photosynthetic induction strongly increased with CO_2 partial pressure, due to increased apparent Rubisco activation rates and reduced diffusional limitations. High leaf temperature produced slightly higher induction rates, and increased intrinsic water use efficiency and diffusional limitation. High $VPD_{leaf\text{-}air}$ slowed down induction rates and apparent Rubisco activation and (at 2·3 kPa) induced damped stomatal oscillations. Blue irradiance had no effect. Slower apparent Rubisco activation in elevated $VPD_{leaf\text{-}air}$ may be explained by low leaf internal CO_2 partial pressure at the beginning of induction.
• **Conclusions** The environmental factors CO_2 partial pressure, temperature and $VPD_{leaf\text{-}air}$ had significant impacts on rates of photosynthetic induction, as well as on underlying diffusional, carboxylation and electron transport processes. Furthermore, maximizing Rubisco activation rates would increase photosynthesis by at most 6–8 % in ambient CO_2 partial pressure (across temperatures and humidities), while maximizing rates of stomatal opening would increase photosynthesis by at most 1–3 %.

Key words: Dynamic photosynthesis, CO_2 concentration, temperature, humidity, stomatal conductance, diffusional limitation, Rubisco, tomato, *Solanum lycopersicum*.

INTRODUCTION

When a dark-adapted leaf is illuminated, photosynthesis (A) starts, and increases over a period of time to a stable steady-state rate. This process, photosynthetic induction, was discovered almost a century ago (Osterhout and Haas, 1918), and its underlying mechanisms have been studied extensively (Pearcy and Way, 2012; Kaiser *et al*., 2016). The main mechanisms that affect photosynthetic induction, and A in fluctuating irradiance, are activation of Calvin cycle enzymes and stomatal opening (Pearcy *et al*., 1996). Additionally, the history of irradiance intensity, plant functional type and environmental conditions modulate the amplitude and kinetics of photosynthetic induction. While previous studies (reviewed in Kaiser *et al*., 2015) have shown that environmental factors such as leaf external CO_2 partial pressure (C_a), leaf temperature (T_{leaf}), leaf-to-air vapour pressure deficit ($VPD_{leaf\text{-}air}$) and blue irradiance can modulate the responses of A to variable irradiance, no study has systematically compared the effects of all of these factors on the photosynthetic response to dark–light transitions.

Due to the wind-induced movement of leaves, canopies and clouds, irradiance incident on a leaf can fluctuate, often resulting in time-dependent changes in A and reductions in irradiance use efficiency compared to the theoretical situation of instantaneous changes in assimilation. Currently, there is renewed interest in the dynamic components of photosynthesis, as (1) faster activation of Rubisco could increase resource use efficiency and productivity (Carmo-Silva *et al*., 2015), (2) stomata that react faster to changes in irradiance could increase intrinsic water use efficiency (WUE_i; Lawson and Blatt, 2014), (3) faster relaxation of non-photochemical quenching (NPQ) could increase photosynthetic quantum yield in limiting irradiance (Murchie and Niyogi, 2011) and (4) predictions of assimilation that account for dynamics could lead to more accurate forecasts of plant productivity (Kaiser *et al*., 2015). To address these questions, the behaviour of dynamic photosynthesis in C_3 crops must be thoroughly understood. However, most effort has been directed towards understorey shrubs and trees, and only a few studies have investigated dynamic photosynthesis and its environmental modulation in C_3 species with high photosynthetic capacity (Yamori *et al*., 2012; Carmo-Silva and Salvucci, 2013; Soleh *et al*., 2016). Such experiments are necessary to quantify limitations to dynamic photosynthesis and to assess how each limiting factor is affected by environmental conditions.

The enzymes that regenerate ribulose-1,5-bisphosphate (RuBP) are activated rapidly during photosynthetic induction (Sassenrath-Cole and Pearcy, 1992). Consequently, RuBP supply to Rubisco is considered to be non-limiting after the first minute of induction (Woodrow and Mott, 1989; Pearcy *et al*., 1996). Rubisco itself typically takes 7–10 min to fully activate *in vivo* (Pearcy *et al*., 1996), and the extent of its limitation during photosynthetic induction and the apparent time constant of its activation (τ_R) can be calculated from gas exchange data (Woodrow and Mott 1989). A low stomatal conductance (g_s) can impose an additional diffusional limitation on induction. By estimating the assimilation rate that would occur if CO_2 partial pressure in the chloroplast (C_c) were identical to C_a (i.e. leaf conductance being infinite), the diffusional limitation acting on transient and steady-state A can be quantified. This diffusional limitation normally includes a component in the mesophyll, which is quantified as mesophyll conductance (g_m). Mesophyll conductance may vary with irradiance, C_a and temperature (Flexas *et al*., 2007, 2008; von Caemmerer and Evans, 2015). However, to our knowledge, no study has examined possible changes of g_m during induction and their implications on diffusional limitation.

During photosynthetic induction, electron and proton transport processes undergo rapid changes, affecting the efficiency of electron transport through photosystem II (Φ_{PSII}) and NPQ. As in the case of steady-state A, linear electron transport rate (ETR) correlates linearly with gross photosynthesis (A_{gr}) during induction (Košvancová-Zitova *et al*., 2009; Yamori *et al*., 2012), and changes in the slope of this relationship can be used to infer changes in photorespiration. NPQ often overshoots at the start of induction (e.g. Johnson *et al*., 1994), which is probably due to the decrease of lumen pH that develops when ETR is limited by low photosynthetic metabolic activity. Hence, measuring Φ_{PSII} and NPQ concurrent with gas exchange can provide detailed information on processes affecting photosynthetic induction.

Dynamic A and its modulation by environmental factors must be better understood in order to improve it. Tomato (*Solanum lycopersicum*), a C_3 model species with intermediate leaf photosynthetic capacity and an important crop in open field and protected cultivation, was used in this study. During photosynthetic induction after a dark–light transition, it was shown how transient diffusional and biochemical limitations, stomatal and mesophyll conductance, apparent Rubisco activation, WUE_i and electron transport processes are affected by C_a, T_{leaf}, $VPD_{leaf\text{-}air}$ and blue irradiance. The benefits and costs of faster Rubisco activation or stomatal opening on dynamic photosynthesis are discussed.

MATERIALS AND METHODS

Plant material

Tomato seeds (*Solanum lycopersicum* 'Cappricia'; Rijk Zwaan, De Lier, the Netherlands) were germinated in Rockwool plugs (Grodan, Roermond, the Netherlands), which after 1 week were transferred to Rockwool cubes (10 cm × 10 cm × 7 cm; Grodan). Plants were grown in a climate chamber with 16/8-h photoperiod, 22/20 °C (day/night) temperature, 70 % relative humidity and 320 µmol m^{-2} s^{-1} photosynthetically active radiation (PAR), measured at table height. Irradiance was provided by a mixture of white, red and far-red LEDs with emission peaks at 440, 550, 660 and 735 nm. Rockwool cubes were standing in a layer (height: 1–2 cm) of nutrient solution (Yara Benelux B.V., Vlaardingen, the Netherlands), which was replenished every 1–2 d and contained 12·4 mM NO_3^-, 7·2 mM K^+, 4·1 mM Ca^{2+}, 3·3 mM SO_4^{2-}, 1·8 mM Mg^{2+}, 1·2 mM NH_4^+, 1·1 mM PO_4^{3-}, 30 µM BO_3^{3-}, 25 µM Fe^{3+}, 10 µM Mn^{2+}, 5 µM Zn^{2+}, 0·75 µM Cu^{2+} and 0·5 µM MoO_4^{2-} (EC 2·1 dS m^{-1}, pH 5·5). When plants were between 5 and 6 weeks old, leaves 4 and 5, counting from the bottom, were used for measurements. At this stage, growth of these leaves was almost complete (data not shown).

Gas exchange and chlorophyll fluorescence measurements

All measurements were performed using the LI-6400 photosynthesis system (Li-Cor Biosciences, Lincoln, NB, USA) equipped with the leaf chamber fluorometer (Li-Cor Part No. 6400-40, area 2 cm^2).

Photosynthetic induction. To assess the response of gas exchange to a step increase in irradiance, leaves were first dark-adapted at the treatment levels described below until g_s was constant (60–120 min). Then, irradiance was increased to 1000 µmol m^{-2} s^{-1} in a stepwise change and gas exchange values were logged every second for 60 min. Although such a dark–light transition does not resemble a natural situation, we chose these extreme irradiance levels in an attempt to maximize the effect of the treatment levels (see below) on photosynthetic induction. An irradiance of 1000 µmol m^{-2} s^{-1} was ∼5 % below saturation, which was a compromise between using a fully saturating irradiance (determined in pilot experiments, see Supplementary Data File S1) and the desire to avoid photoinhibition of photosynthesis. The flow rate of air was 500 µmol s^{-1}. Other than when adjusted as part of a treatment, the standard conditions in the cuvette were: 39·7–40·3 Pa C_a (range of lowest to highest value), 0·7–1·0 kPa $VPD_{leaf\text{-}air}$, 22·3–23·3 °C T_{leaf} and 90:10 % red/blue irradiance mixture provided by LEDs. The values of all cuvette conditions reported here are averages over whole induction curves. Peak intensities of red and blue LEDs were at wavelengths of 635 and 465 nm, respectively. Treatments were applied individually and included: 20, 40 and 80 Pa C_a, 15·5, 22·8 and 30·5 °C T_{leaf}, 0·5, 0·8, 1·6 and 2·3 kPa $VPD_{leaf\text{-}air}$ (0·4, 0·9, 1·7 and 2·5 VPD_{air}) and 0, 1, 5, 10 and 20 % blue irradiance in a red irradiance background. For each treatment, five biological replicates were used ($n = 5$). All measurements were performed in a lab except the 15·5 and 30·5 °C T_{leaf} treatments, which were performed in climate chambers. Despite efforts to keep $VPD_{leaf\text{-}air}$ similar between T_{leaf} treatments, it was, on average, 0·97 kPa at 15·5 °C, 0·80 kPa at 22·8 °C and 0·84 at 30·5 °C (Supplementary Data File S2). Transient A_n, g_s and C_i were averaged over five data points using a moving average filter to reduce measurement noise. Assimilation was corrected for CO_2 leaks using dried leaves (Long and Bernacchi, 2003).

To analyse the effect of C_a and T_{leaf} on photosynthetic electron transport processes, another set of induction curves was performed on different leaves, with the same cuvette conditions as described above. ETR was estimated from measurements of

Φ_{PSII}, which was calculated from measurements of F_s (fluorescence yield under continuous actinic irradiance) and F_m' (maximum fluorescence yield during a saturating irradiance pulse). The measurements of F_m' were also used to calculate NPQ according to the Stern–Volmer quenching model (i.e. as $1 - F_m/F_m'$) and using F_m from dark-adapted leaves. Measurements of F_m' were made once a minute during the first 10 min of induction, and once every 2 min thereafter. To ensure the accurate measurement of F_m', the multi-phase flash (MPF) protocol of the Li-Cor fluorometer was used (Loriaux *et al.*, 2013). Using MPFs instead of single saturating pulses prevents underestimation of maximum chlorophyll fluorescence yield in light-adapted leaves of high photosynthetic capacity. F_m' estimated by the MPF was ~4 % larger than measured F_m' (Supplementary Data File S3). Settings of the MPF were determined in preliminary measurements. These were 8500 and 1–2 µmol m^{-2} s^{-1} flash and measuring beam intensity, respectively; 60 % decrease of flash intensity during the 2nd phase of the MPF; and 0·3, 0·7 and 0·4 s duration of the three flash phases. These settings yielded high correlations ($R^2 \approx 0{\cdot}99$) between flash intensity and F_m' during flash phase 2 after the first or second minute of induction (data not shown). Preliminary data indicated limited effects of $VPD_{leaf\text{-}air}$ on Φ_{PSII} or NPQ (data not shown); therefore, those measurements were not repeated here.

A/C$_i$ curves. To estimate the parameters V_{Cmax}, ETR_{max}, TPU and Γ*, A/C_i curves were first performed in photorespiratory and then in non-photorespiratory conditions (21 and 2 kPa oxygen, respectively; Supplementary Data File S4). Leaves were first adapted to 50 Pa CO_2 and 21 kPa O_2 for ~30 min, then CO_2 partial pressure was reduced in a stepwise manner until 5 Pa, each step taking ~4 min. Then, CO_2 was again raised to 50 Pa for ~15 min, after which it was increased to 150 Pa in several steps, each step taking ~5 min. Then, O_2 partial pressure was reduced to 2 kPa, and the procedure was repeated. Altogether, A was logged at 11 CO_2 partial pressures per O_2 partial pressure, and each complete A/C_i curve took ~2·5 h. Data were logged every 5 s, and averages of 10 values at each C_a step, after steady-state A had visibly been reached, were used. Other cuvette conditions were: 1000 µmol m^{-2} s^{-1} PAR, 0·8 kPa $VPD_{leaf\text{-}air}$ and 23 °C T_{leaf}.

A/PAR curves. To estimate parameters R_d and s (lumped parameter used to scale the product of irradiance and Φ_{PSII} onto ETR), irradiance-limited curves were performed in 2 % oxygen [File S4]. The intercept of the linear $A/(PAR \times \Phi_{PSII} \times 0{\cdot}25)$ relationship was R_d, while the slope was s (Yin *et al.*, 2009). Leaves were adapted to 200 µmol m^{-2} s^{-1}, until A and g_s were stable. Then, leaves were exposed to a range of PAR values between 0 and 200 µmol m^{-2} s^{-1}. Assimilation was determined as described for the A/C_i curves. Φ_{PSII} was determined as described above. Other cuvette conditions were: 40 Pa C_a, 0·8 kPa $VPD_{leaf\text{-}air}$ and 22 °C T_{leaf}.

Calculations

All calculations described here were performed on single replicates, and then used for further (statistical) analysis. Photosynthetic induction was calculated after Chazdon and Pearcy (1986): transient A (µmol m^{-2} s^{-1}) was expressed as a percentage of the final rate (A_f), corrected for the initial, dark-adapted rate (A_i)

$$Photosynthetic\ induction = \frac{A - A_i}{A_f - A_i} \cdot 100 \qquad (1)$$

The relative rate of increase of g_s (mol m^{-2} s^{-1}) during induction was calculated similarly. For the calculation of several parameters, gas exchange data were corrected for transient changes in C_i or C_c (using g_m as in Table 1 in Supplementary Data File S5) during induction. For diffusional limitation (LD; %), A was multiplied by the percentage by which A would increase if CO_2 partial pressure in the chloroplast (C_c, Pa) during induction was equal to leaf external partial pressure, C_a ($A^*_{C_a}$). For biochemical limitation (LB; %) and the apparent rate constant of Rubisco activation (τ_R; min), A was multiplied by the percentage by which A would increase if transient C_i was similar to final, steady-state C_i ($A^*_{C_i}$), following Woodrow and Mott (1989). However, unlike Woodrow and Mott (1989), for calculations of $A^*_{C_a}$ and $A^*_{C_i}$ no linear relationship between C_i and the CO_2 compensation point (Γ*, Pa) was assumed. Instead, information from complete A/C_i curves was used to correct A using the steady-state, curvilinear response of A to C_i. In the case of $A^*_{C_a}$, A was corrected for the minimum of either Rubisco activity-limited A (A_c), RuBP-limited A (A_j) or triose phosphate utilization-limited A (A_t) at C_a (in the numerator) and at C_c (in the denominator):

$$A^*_{C_a} = A \cdot \frac{min\{A_c(C_a),\ \ A_j(C_a),\ \ A_t(C_a)\}}{min\{A_c(C_c),\ \ A_j(C_c),\ \ A_t(C_c)\}} \qquad (2)$$

A_c, A_j and A_t were calculated after the FvCB model (Farquhar *et al.*, 1980) modified to account for TPU limitation (Sharkey 1985). In eqns (3)–(5), the calculations for A at C_a are shown. For calculating A at C_c, C_i or C_{if}, C_a was replaced by any of these variables (not shown here):

$$A_c(C_a) = V_{Cmax}\left(\frac{C_a - \Gamma^*}{C_a + \ K_c \ \cdot \ \left(1 + \frac{O}{K_o}\right)}\right) - R_d \qquad (3)$$

$$A_j(C_a) = ETR_{max}\left(\frac{C_a - \Gamma^*}{4 \ \cdot \ C_a + \ 8 \ \cdot \ \Gamma^*}\right) - R_d \qquad (4)$$

$$A_t(C_a) = 3 \cdot TPU - R_d \qquad (5)$$

where V_{Cmax} (µmol m^{-2} s^{-1}) is maximum velocity of Rubisco for carboxylation, R_d is day respiration (µmol m^{-2} s^{-1}), O (kPa) is the chloroplast O_2 partial pressure, K_c (Pa) and K_o (kPa) are the Michaelis-Menten constants of Rubisco for CO_2 and for O_2, respectively, ETR_{max} (µmol m^{-2} s^{-1}) is the maximum rate of electron transport in the absence of regulation and TPU (µmol m^{-2} s^{-1}) is the triose phosphate utilization rate. Parameters V_{Cmax}, ETR_{max} and TPU were estimated using the Excel routine of Sharkey *et al.* (2007). The first five points of A/C_i curves at 21 kPa O_2 partial pressure were used to estimate V_{Cmax} (initial slope), the next four points to estimate ETR_{max} and the uppermost two points to estimate TPU (n=3). R_d and Γ* were determined after Yin *et al.* (2009). Additionally, R_d was corrected for

TABLE 1. *Parameters used in the calculations of diffusional limitation, biochemical limitation and the apparent time constant of Rubisco (eqns 3–5)*

Parameter	Unit	Temperature (°C)		
		15·5	22·8	30·5
ETR_{max}	µmol m^{-2} s^{-1}	94·33	148·16	232·97
K_c	Pa	9·29	21·36	49·25
K_o	kPa	12·04	15·37	19·63
R_d	µmol m^{-2} s^{-1}	0·77	1·23	2·00
TPU	µmol m^{-2} s^{-1}	5·98	10·32	17·84
V_{Cmax}	µmol m^{-2} s^{-1}	43·35	84·86	166·44
Γ*	Pa	3·62	5·34	7·88

Parameters ETR_{max}, TPU and V_{Cmax} were determined from A/C_i curves after Sharkey *et al*. (2007), K_c and K_o were taken from Sharkey *et al*. (2007), R_d and Γ* were determined from A/PAR and A/C_i curves after Yin *et al*. (2009). All parameters were temperature-adjusted after Bernacchi *et al*. (2001).

respiration under the gasket of the gas exchange cuvette (Pons and Welschen, 2002). Parameters K_c and K_o were taken from Sharkey *et al*. (2007). All parameters were temperature-adjusted (Bernacchi *et al*., 2001); their values are given in Table 1. We acknowledge that the use of a steady-state model to correct A during transients may be inaccurate (e.g. V_{Cmax} and J_{max} change during induction; Soleh *et al*., 2016), and that further work should be dedicated to refining this method. LD was determined by analogy to stomatal limitation as in Urban *et al*. (2007):

$$LD = \frac{A^*_{C_a} - A}{A_f - A_i} \cdot 100 \quad (6)$$

LB was calculated by using $A^*_{C_i}$, i.e. final steady-state C_i (C_{if}) in the numerator and C_i in the denominator of eqn (2) instead of C_a and C_c, respectively. LB was calculated after Urban *et al*. (2007):

$$LB = \frac{A_f - A^*_{C_i}}{A_f - A_i} \cdot 100 \quad (7)$$

τ_R was calculated after Woodrow and Mott (1989):

$$\tau_R = \frac{\Delta time}{\Delta \ln \cdot (A_i - A^*_{C_i})} \quad (8)$$

For the C_a and $VPD_{leaf\text{-}air}$ treatments, data from minutes 2–5 during induction were used for Δtime [it has been determined by Woodrow and Mott (1989) that during this phase Rubisco activation is the main limiting factor], while in the case of varying T_{leaf}, data were taken from minutes 5–8 during induction, to account for a possible slower activation of RuBP regeneration in the beginning of induction due to low T_{leaf}. WUE_i (µmol $mmol^{-1}$) was calculated as:

$$WUE_i = \frac{A}{g_s} \quad (9)$$

Φ_{PSII} and NPQ were calculated after Genty *et al*. (1989) and Bilger and Björkman (1991), respectively. The coefficient of photochemical quenching (q_P) and PSII maximum efficiency (F_v'/F_m') was calculated after Oxborough and Baker (1997). ETR was calculated after Yin *et al*. (2009):

$$ETR = \Phi_{PSII} \cdot PAR \cdot s \quad (10)$$

where s is a unitless lumped calibration factor used to scale Φ_{PSII} to ETR (Yin *et al*., 2009). The maximum change in A (in percent) that would occur if either Rubisco instantly became fully activated or g_s immediately reached its final steady-state level (g_{sf}, Table 2) directly after the onset of illumination was calculated as the average of LB and LD between minutes 2 and 60 during induction, respectively. LB and LD data from the first minute after the onset of illumination were left out, as the activation of RuBP regeneration is known to be the main limiting factor of photosynthetic induction during that phase (Pearcy *et al*., 1996). The changes in WUE_i (in percent) were calculated as:

$$WUE_{iinstantRubisco} = \left(\frac{\frac{A_f}{g_s} - WUE_i}{WUE_{if}} \right) * 100 \quad (11)$$

and

$$WUE_{iinstantgs} = \left(\frac{\frac{A}{g_{sf}} - WUE_i}{WUE_{if}} \right) * 100 \quad (12)$$

after which their averages during minutes 2–60 were determined. $WUE_{i\_instantRubisco}$ and $WUE_{i\_instantgs}$ are the changes in WUE_i that would occur if Rubisco became immediately fully activated, or g_s increased immediately to its final value. WUE_{if} is final, steady-state WUE_i.

Statistical analysis

Most data are expressed as mean ± standard error (SE). Parameters shown in Table 2 and in Fig. 4 were tested for normality (Shapiro-Wilk test; Genstat 16th edn, VSN International, Hempstead, UK) and homogeneity of variances (Fligner–Killeen test; R, R Core Team). On datasets where those requirements were fulfilled, one-way analysis of variance (ANOVA; Genstat) was performed, followed by Fisher's protected LSD (Genstat) to determine significant differences between treatments. When datasets did not meet the requirement of normality or homogeneity of variances, they were log-transformed. On datasets where homogeneity of variances could be assumed, but the requirement of normality was not fulfilled, a non-parametric Kruskal–Wallis (Genstat) test was conducted.

RESULTS

Induction of photosynthetic CO_2 fixation

Rates of photosynthetic induction increased with C_a (Fig. 1A), affecting the time to reach 50 and 90 % of full induction (t_{A50} and t_{A90}, respectively), but not induction 60 s after illumination (IS_{60}; Table 2). High T_{leaf} (30·5 °C) increased induction slightly

TABLE 2. *Dynamic and steady-state parameters of photosynthetic induction in tomato leaves, as affected by* C_a, T_{leaf}, $VPD_{leaf\text{-}air}$ *and blue light*

Treatment	Dynamic parameters					Mean at start and end of induction			
	IS_{60}	t_{A50}	t_{A90}	t_{gs50}	t_{gs90}	A_i	A_f	g_{si}	g_{sf}
20 Pa	25·7 ± 3·0	3·2 ± 0·6b	18·5 ± 4·0b*	19·8 ± 1·2	46·7 ± 1·4b	−1·1 ± 0·6	11·7 ± 1·3a	0·22 ± 0·04	0·65 ± 0·05c
40 Pa	21·6 ± 2·7	2·6 ± 0·2a	10·8 ± 1·4ab*	18·7 ± 3·1	38·2 ± 5·6a	−1·6 ± 0·3	22·2 ± 1·4b	0·27 ± 0·06	0·56 ± 0·07b
80 Pa	21·9 ± 4·4	2·2 ± 0·3a	6·2 ± 0·3a*	18·2 ± 2·2	39·9 ± 4·7a	−1·3 ± 0·6	27·1 ± 2·3c	0·25 ± 0·06	0·46 ± 0·07a
15·5 °C	15·8 ± 4·5a*	2·7 ± 0·3b	12·6 ± 1·4	24·4 ± 4·8	42·5 ± 1·4	−1·1 ± 0·3b	15·6 ± 2·2a †	0·17 ± 0·16a	0·34 ± 0·14a
22·8 °C	21·6 ± 2·7b*	2·6 ± 0·2b	10·8 ± 1·4	18·7 ± 3·1	38·2 ± 5·6	−1·6 ± 0·3ab	22·2 ± 1·4b †	0·27 ± 0·06b	0·56 ± 0·07b
30·5 °C	37·8 ± 7·8c*	1·6 ± 0·4a	13·4 ± 1·6	17·2 ± 1·9	34·5 ± 2·2	−2·3 ± 0·5a	21·3 ± 3·8b †	0·21 ± 0·03ab	0·36 ± 0·10a
0·5 kPa	22·3 ± 1·1	2·4 ± 0·8	10·7 ± 1·9A	20·7 ± 0·8b	45·3 ± 15·6c	−1·3 ± 0·1	21·5 ± 0·9	0·30 ± 0·01b	0·57 ± 0·02b
0·8 kPa	21·6 ± 3·9	2·6 ± 0·3	10·8 ± 2·6A	18·7 ± 5·3b	38·2 ± 13·8bc	−1·6 ± 0·8	22·2 ± 1·8	0·27 ± 0·04b	0·56 ± 0·14b
1·6 kPa	24·3 ± 2·7	2·8 ± 0·2	13·5 ± 1·4B	11·7 ± 3·1a	20·2 ± 5·6a	−1·5 ± 0·3	20·0 ± 1·4	0·11 ± 0·06a	0·34 ± 0·07a
2·3 kPa	25·5 ± 1·8	3·1 ± 0·1	11·5 ± 5·2Ab	8·7 ± 4·5a	31·2 ± 7·2ab	−1·7 ± 0·5	19·4 ± 0·7	0·09 ± 0·05a	0·26 ± 0·05a
0 % blue irradiance	24·6 ± 4·4	2·5 ± 0·4	13·8 ± 2·1	17·5 ± 3·1	33·2 ± 6·7	−1·7 ± 0·4	20·5 ± 1·3	0·19 ± 0·07	0·42 ± 0·07
1 % blue irradiance	23·0 ± 4·3	2·7 ± 0·3	13·0 ± 1·4	15·3 ± 3·8	30·8 ± 9·2	−1·9 ± 0·5	20·9 ± 2·1	0·16 ± 0·04	0·46 ± 0·08
5 % blue irradiance	21·5 ± 6·4	2·7 ± 0·3	14·7 ± 3·0	16·8 ± 1·8	35·2 ± 5·5	−2·2 ± 0·4	20·9 ± 1·7	0·17 ± 0·08	0·45 ± 0·09
10 % blue irradiance	21·6 ± 2·7	2·6 ± 0·2	10·8 ± 1·4	18·7 ± 3·1	38·2 ± 5·6	−1·6 ± 0·3	22·2 ± 1·4	0·27 ± 0·06	0·56 ± 0·07
20 % blue irradiance	18·6 ± 5·3	2·7 ± 0·4	12·4 ± 1·2	18·2 ± 1·3	37·6 ± 2·8	−1·4 ± 0·6	22·0 ± 2·5	0·22 ± 0·07	0·51 ± 0·09

Dynamic parameters include IS_{60} (induction 60 s after illumination, %), t_{A50}, t_{A90}, t_{gs50} and t_{gs90} [time (min) to reach 50 and 90 % of photosynthetic induction and time to reach 50 and 90 % of full stomatal opening]. Steady-state parameters were calculated by averaging single values over 2 min (either in dark-adapted leaves or at the end of induction) and include A_i, A_f, g_{si} and g_{sf} (A and g_s in darkness and in 1000 μmol m^{-2} s^{-1}, respectively; units: A expressed in μmol m^{-2} s^{-1} and g_s in mol m^{-2} s^{-1}). Means followed by different letters differ significantly, according to a LSD test conducted at the $P = 0{\cdot}05$ level ($n = 5$); absence of letters denotes absence of significant effects.

*One-way ANOVA performed on log-transformed data.

†Data compared using non-parametric Kruskal–Wallis test.

in the first 5 min (Fig. 1C), affecting IS_{60} and t_{A50} but not t_{A90} (Table 2). Elevated $VPD_{leaf\text{-}air}$ slowed down induction after ~5 min (Fig. 1E), increasing t_{A90} in 1·6 kPa (Table 2). High $VPD_{leaf\text{-}air}$ (2·3 kPa) induced oscillations of induction rates (Fig. 1E), without affecting the various induction parameters. However, it is difficult to determine those parameters in an oscillating time series. Varying blue irradiance (0–20 %) did not affect any parameter in Table 2, nor did it have noticeable effects on other parameters discussed here (data not shown).

Stomatal conductance

Stomata opened faster in low C_a (Fig. 1B) and reached higher final conductance (g_{sf}, Table 2). However, because g_s levelled off earlier in intermediate and high C_a, the time to reach 90 % of full stomatal conductance (t_{gs90}) was significantly longer in low C_a (Table 2). Low (15·5 °C) and high T_{leaf} decreased g_s in darkness (g_{si}, Table 2) and decreased the extent of stomatal opening during induction (Fig. 1D), leading to lower steady-state g_{sf} compared to intermediate T_{leaf} (22·8 °C). Elevated $VPD_{leaf\text{-}air}$ affected stomata by (1) decreasing g_{si} and g_{sf}, (2) increasing relative opening rates in the first 15 min of induction, (3) inducing damped stomatal oscillations at the highest $VPD_{leaf\text{-}air}$ (2·3 kPa) and (4) causing stomata to reach steady-state g_s more quickly (or quasi steady-state in the case of an oscillating g_s; Fig. 1F, Table 2). Despite decreasing g_{si} by 40–55 % compared to low $VPD_{leaf\text{-}air}$, high $VPD_{leaf\text{-}air}$ did not affect final A (A_f; Table 2), suggesting that in the steady state, diffusional limitation of A was no longer sensitive to $VPD_{leaf\text{-}air}$. Time courses of C_c during photosynthetic induction are shown in Supplementary Data File S6.

Intrinsic water use efficiency (WUE_i)

WUE_i, a result of dynamic changes in A and g_s, was strongly affected by C_a: both its steady-state level and its rate of change in the first 30 min of induction were increased in high compared to low C_a (Fig. 2A). At low and high T_{leaf}, g_s increased more slowly, with similar increases in A, in the beginning of induction, so both resulted in a higher WUE_i than for an intermediate T_{leaf} (Fig. 2B). A similar reasoning applies to $VPD_{leaf\text{-}air}$: because elevated $VPD_{leaf\text{-}air}$ reduced g_s more strongly than A during and after induction, WUE_i was highest in 2·3 kPa, followed by 1·6 kPa (Fig 2C). The 0·5- and 0·8-kPa treatments showed lowest WUE_i and were no different from each other (Fig. 2C).

Diffusional and biochemical limitations during photosynthetic induction

Diffusional limitation quantifies the reduction in A due to C_c being lower than C_a. This is a complex parameter that depends on the combined effects of C_a, A and total leaf diffusive conductance on C_c, as well as the extent to which C_c imposes a limitation on A. Biochemical limitation quantifies the extent to which biochemical processes that activate during induction limit A during induction, but not in the steady state. Note that the sum of these limitations is not 100 %, as they are calculated not with respect to the total limitation for A, but to reference gaseous diffusion and biochemical states. In all treatments except at high VPD (2·3 kPa), transient diffusional limitation increased to its maximum within the first 15 min due to the activation of Rubisco, and then slowly relaxed to its steady-state level as stomata opened. Biochemical limitation was at its

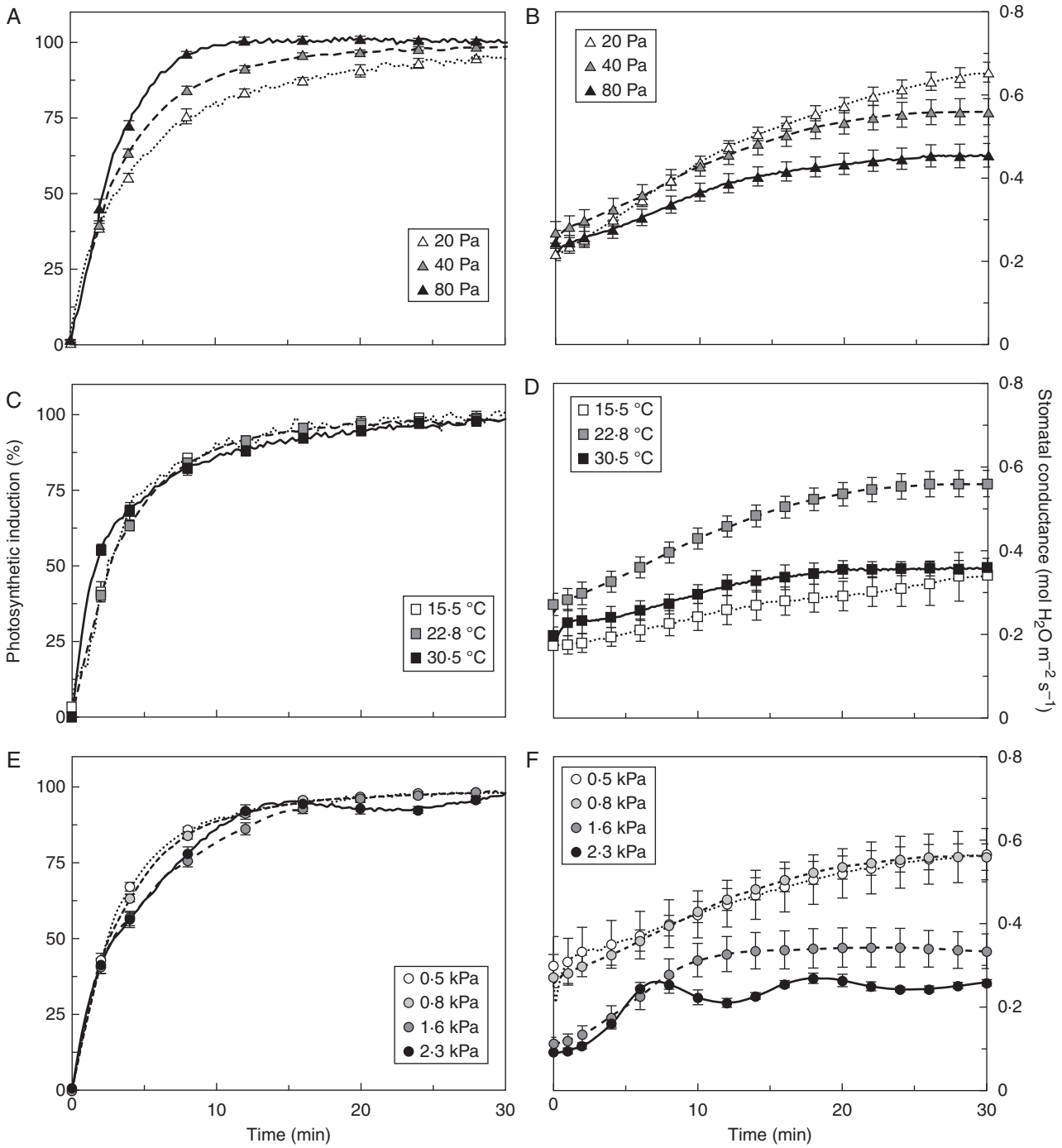

FIG. 1. Photosynthetic induction (A, C, E) and stomatal conductance (B, D, F) in dark-adapted tomato leaves, as affected by C_a (A, B), T_{leaf} (C, D) and $VPD_{leaf\text{-}air}$ (E, F). Irradiance was raised from 0 to 1000 μmol m^{-2} s^{-1} at time = 0 and kept steady for 60 min. In A, C and E, the first 30 min of induction are shown. Mean ± SE ($n = 5$).

maximum in the very beginning of induction, and relaxed rapidly within the first 10–15 min. The extent, as well as the rates, of buildup and relaxation of diffusional and biochemical limitation scaled negatively with C_a (Fig. 3A, B). Diffusional limitation was higher in low compared to intermediate C_a, while there was no difference in biochemical limitation between these treatments. High C_a decreased the diffusional limitation and produced a faster relaxation of biochemical limitation than both low and intermediate C_a (Fig. 3A, B). When biochemical limitation had relaxed entirely at high C_a (~10 min), ~10 % of biochemical limitation remained at intermediate and low C_a, taking another 10 min to relax (Fig. 3B). High T_{leaf} induced strong diffusional limitation (Fig. 3C), while maintaining slightly positive effects on the rates of relaxation of

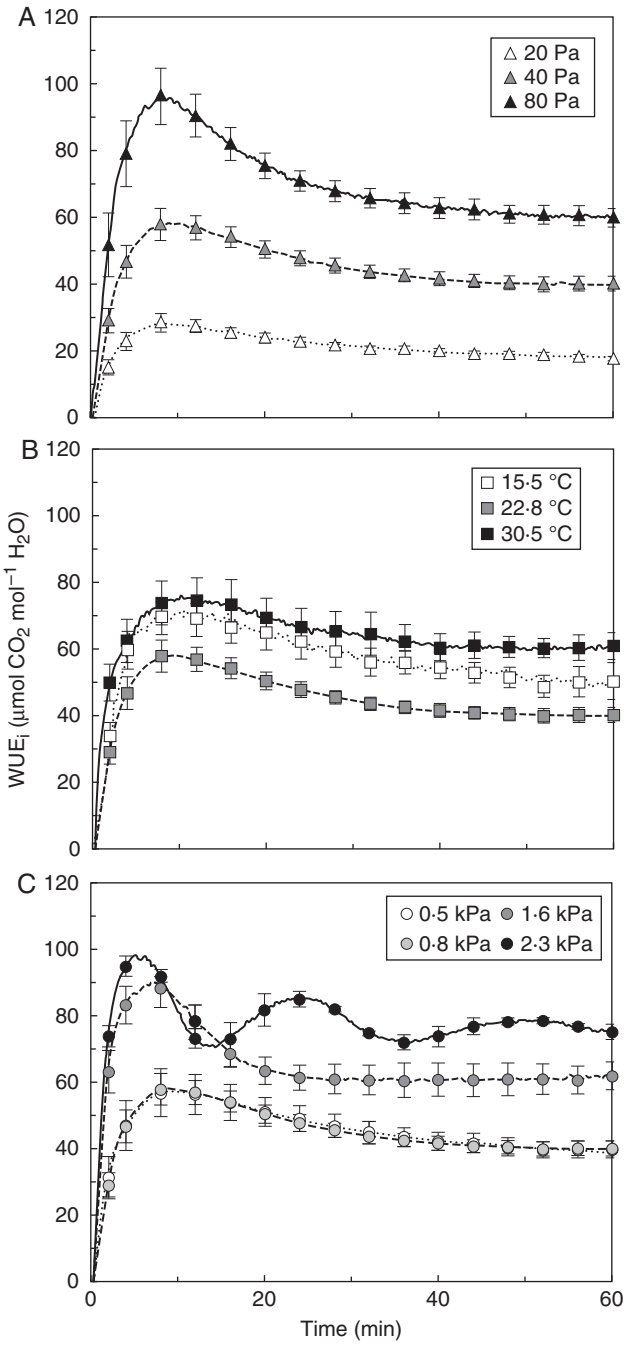

FIG. 2. Intrinsic water use efficiency (WUE_i) during photosynthetic induction, as affected by C_a (A), T_{leaf} (B) and $VPD_{leaf\text{-}air}$ (C). Mean ± SE ($n = 5$).

biochemical limitation (Fig. 3D). The effects of high $VPD_{leaf\text{-}air}$ (1·6 and 2·3 kPa) on g_s translated into very different kinetics of diffusional limitations during induction than moderate $VPD_{leaf\text{-}air}$. The 1·6-kPa treatment led to a faster decrease in diffusional limitation than 0·5 or 0·8 kPa, while 2·3 kPa produced an oscillating diffusional limitation (Fig. 3E). Biochemical limitation was affected less strongly, although it tended to relax more slowly in elevated $VPD_{leaf\text{-}air}$ (Fig. 3F).

Apparent time constants of Rubisco activation

The apparent time constant for Rubisco activation (τ_R), defined as the time to reach 63 % of final Rubisco activation, decreased with increasing C_a (Fig. 4A), reflecting faster activation of Rubisco with larger abundance of CO_2. Compared to τ_R in low C_a, τ_R at intermediate and high C_a was 20 and 56 % lower, respectively. Leaf temperature did not have a statistically significant effect on τ_R, although there was a trend towards higher τ_R in low T_{leaf} (Fig. 4B). Elevated $VPD_{leaf\text{-}air}$ significantly increased τ_R, by 45 and 48 % in the 1·6- and 2·3-kPa treatments (compared with 0·5 kPa; Fig. 4C).

Slower apparent Rubisco activation in elevated $VPD_{leaf\text{-}air}$ (compared to low $VPD_{leaf\text{-}air}$) was probably related to lower values of C_i, due to the lower g_s at high $VPD_{leaf\text{-}air}$. The decrease in C_i at the start of induction was stronger in elevated compared to low $VPD_{leaf\text{-}air}$. τ_R tended to increase with the relative rates of decrease in C_i, and data from the C_a treatments showed a similar trend (Fig. 5A), indicating that if C_i depleted too rapidly, apparent Rubisco activation was slowed down. Also, in an attempt to estimate the lowest CO_2 partial pressure reached in the chloroplast, C_c was calculated at the time of induction when C_i reached its lowest point. Plotting τ_R against this C_c, a tendency towards lower τ_R at higher C_c emerged (Fig. 5B), indicating that a very low C_c during induction slows down the activation of Rubisco. Different leaf temperatures could affect the rate of Rubisco activation in addition to their effect on C_i, so they were not taken into account in Fig. 5, which shows only the effect of C_i and C_c on τ_R.

Mesophyll conductance

Mesophyll conductance increased markedly during induction in all treatments, and the fastest changes were observed in the first 10 min of induction. Rates of increase and steady-state levels of g_m were higher at low than at high C_a. At different leaf temperatures, g_m increased with T_{leaf}. Details of dynamic g_m changes and their determination can be found in File S5.

Φ_{PSII} and NPQ during photosynthetic induction

The maximum, dark-adapted quantum efficiency of electron transport through photosystem II (F_v/F_m) ranged between 0·79 and 0·82 across C_a and T_{leaf} treatments. During induction, Φ_{PSII} increased to its steady-state level within 20 min. Between minutes 2 and 14, the relative rates of increase of Φ_{PSII} were significantly higher in high compared to low C_a. Furthermore, steady-state levels of Φ_{PSII} were highest in intermediate C_a (0·35), followed by the high (0·33) and low C_a treatments (0·28; Fig. 6A). During induction, NPQ initially increased towards a peak of ~2 after 5 min. This peak was followed by a decline, which was most pronounced at intermediate C_a (Fig. 6C). The lowest value of NPQ (1·5) was found at intermediate C_a and occurred after ~15 min in all C_a treatments, after which NPQ increased slowly. This last phase was similar at all CO_2 partial pressures, but values of NPQ were highest in low C_a (NPQ of 2), followed by high C_a (1·8) and the lowest value of NPQ (1·7) was found at intermediate C_a (Fig. 6C). Between minutes 2 and 5, high leaf

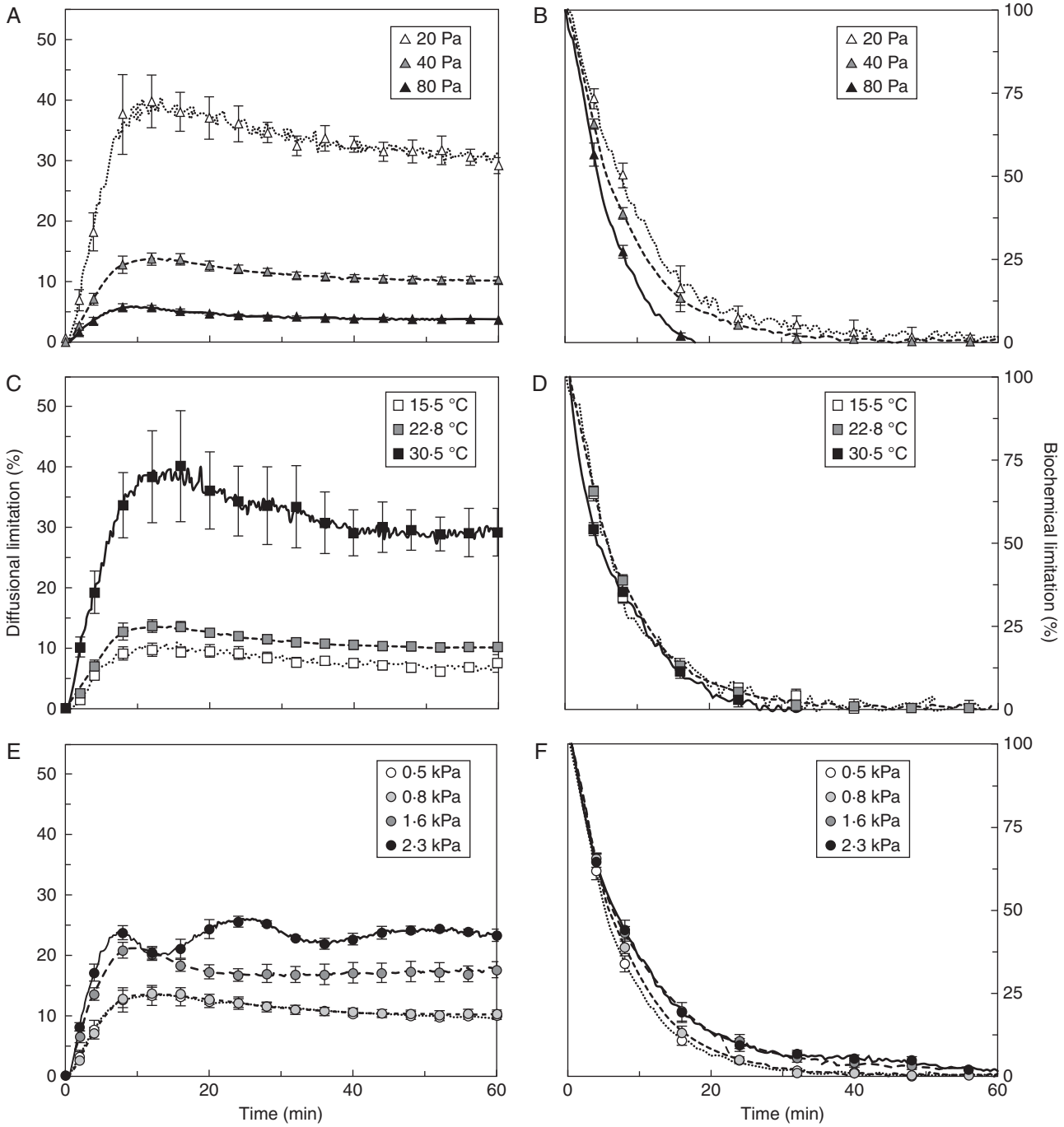

FIG. 3. Diffusional limitation (A, C, E) and biochemical limitation (B, D, F) during photosynthetic induction, as affected by C_a (A, B), T_{leaf} (C, D) and $VPD_{leaf\text{-}air}$ (E, F). In B, D and F, the first 30 min of induction are shown. Mean ± SE ($n = 5$).

temperature increased the relative rate of change of Φ_{PSII} compared to low T_{leaf}. Furthermore, steady-state Φ_{PSII} values scaled positively with T_{leaf}, reaching 0·42 at high, 0·35 at intermediate and 0·22 at low T_{leaf} (Fig. 6B). At intermediate and high T_{leaf} and varying C_a, the time courses of NPQ during induction were similar, rising rapidly to a maximum within 1–4 min, after which there was a decline to a minimum at ~20 min (Fig 6C, D), followed by a rise to the steady-state value, except for the 30·5 °C treatment in which there was a continuous decline (Fig. 6D). At low T_{leaf} the response was different: an initial rapid increase in NPQ was less pronounced and was followed by a slow increase that did not reach a stable value during the experiment. Final NPQ values were therefore highest at low T_{leaf} (~2), followed by intermediate (NPQ of 1·7) and high T_{leaf} (1·3). While changes in q_P paralleled Φ_{PSII} and were of the same magnitude, changes in F_v'/F_m' were rather small (Supplementary Data File S7). As a result, Φ_{PSII} correlated

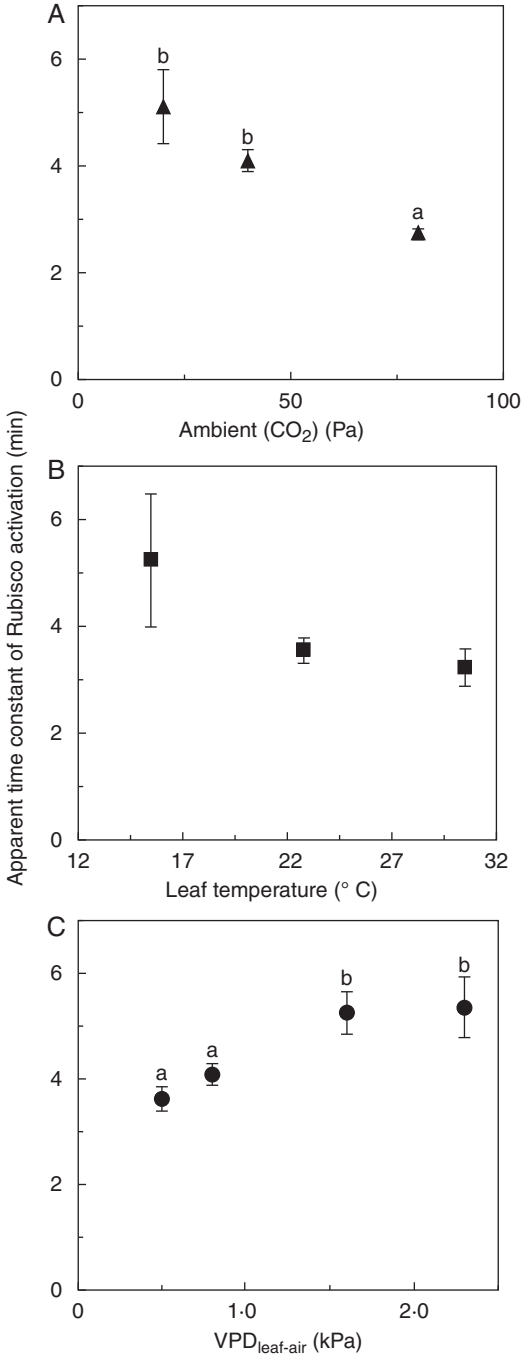

FIG. 4. Apparent time constants of Rubisco activation (τ_R) during photosynthetic induction, as affected by C_a (A), $VPD_{leaf\text{-}air}$ (B) and leaf temperature (C). Small letters denote significant differences between treatments, error bars denote ± SE ($n = 5$).

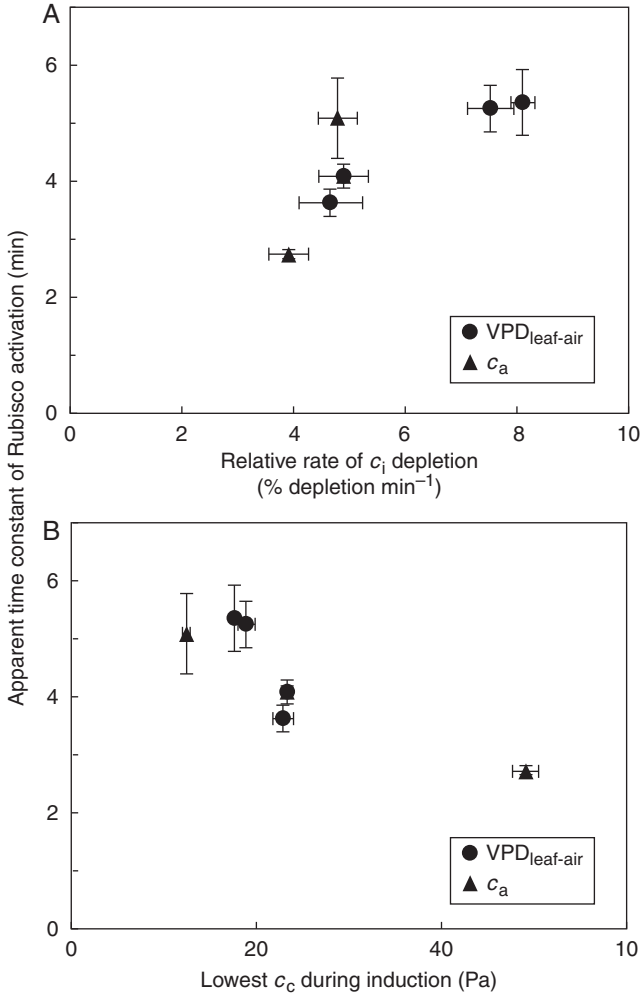

FIG. 5. Relationships between τ_R in the $VPD_{leaf\text{-}air}$ and C_a treatments and (A) the rate of C_i depletion ($\frac{\Delta C_i/\Delta t}{initial\ C_i} * (-100)$), normalized by C_i in darkness (initial C_i) during the first 5 min of induction and (B) the lowest value of C_c during induction, using the lowest value of C_i during induction and corresponding values of A_n and g_m, then calculating $C_c = C_i - \frac{A_n}{g_m}$. Mean ± SE ($n = 5$).

linearly and positively with q_P, while F_v'/F_m' correlated strongly and negatively with NPQ (data not shown).

Electron transport and gross photosynthesis rates

Regressions of gross photosynthesis ($A_{gr} = A_n + R_d$) vs. ETR were predominantly linear (Fig. 7), but the slopes of this relationship increased with C_a and decreased slightly with T_{leaf}. Additionally, at low C_a and at high T_{leaf}, increases in A_{gr} became progressively independent of increases in ETR at high values of ETR and A_{gr}.

DISCUSSION

The environmental factors CO_2 partial pressure, temperature and $VPD_{leaf\text{-}air}$ had significant impacts on rates of photosynthetic induction, and on underlying diffusional, carboxylation and electron transport processes. For the first time, their effects have been compared using the same experimental set-up, and explored in a highly detailed manner. The results indicate the maximum gains that improvements in dynamic photosynthesis would have in various environments and atmospheres.

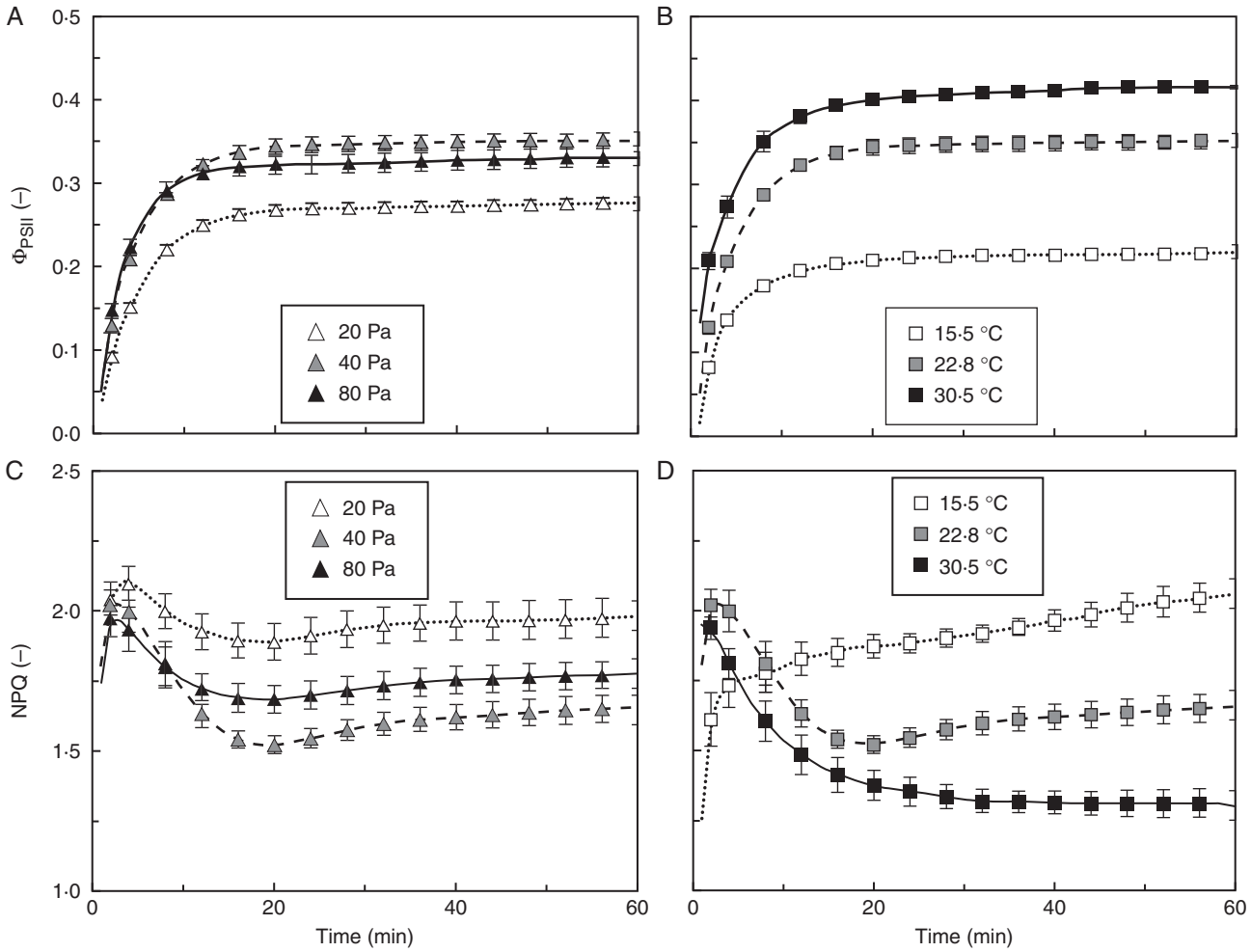

FIG. 6. Changes in Φ_{PSII} (A, B) and NPQ (C, D) during photosynthetic induction, as affected by C_a (A, C) and T_{leaf} (B, D). Mean ± SE ($n = 5$).

CO_2 partial pressure: effects via diffusional and biochemical limitations

By lowering diffusional and biochemical limitations, increased C_a sped up photosynthetic induction considerably. This was reflected in gas exchange (Fig. 1A) and chlorophyll fluorescence data (Fig. 6A, C; discussed below). Despite decreasing g_s and g_m, increased C_a actually lowered diffusional limitation. There are two reasons for this: firstly, due to the curvilinearity of the A/C_c response, a difference between A at C_a and A at C_c (which is the basis of the calculation of diffusional limitation) is larger at low C_a (e.g. 20 Pa) than at high C_a (e.g. 80 Pa). Secondly, the gradient for diffusion between C_a and C_c was steeper (File S6) with increases in C_a, thus decreasing diffusional limitation. A decrease in biochemical limitation was achieved by faster activation of Rubisco (Fig. 4A), but not by faster activation of RuBP regeneration, as visible from the similarity of the initial slopes (Fig. 1A) and the parameter IS_{60} (Table 2). The positive effect of increased C_a on apparent Rubisco activation has been noted before (Mott and Woodrow, 1993; Woodrow *et al*., 1996), and is hypothesized to be due to faster carbamylation of Rubisco.

Because A increased faster and reached a higher value, and g_s increased to a smaller extent, WUE_i was strongly enhanced during and after photosynthetic induction (Fig. 2A) in high C_a. In absolute terms, elevated C_a is positive for WUE_i in fluctuating irradiance. After sudden drops in irradiance, WUE_i decreases quickly as A decreases more quickly than g_s (Lawson and Blatt, 2014). Since g_s is depressed in elevated C_a, the drops in WUE_i after decreases in irradiance are likely to be smaller compared to current atmospheric C_a. Stomatal opening, and the concomitant increase in C_i, decreased the rate of photorespiration in low C_a, as seen from the change in the slope of A_{gr}/ETR (Fig. 7A): when reaching higher values of A_{gr}, this was achieved almost without increases in ETR (i.e. there was a deviation from the previous linear relationship of A_{gr}/ETR), meaning that the rate of oxygenation decreased relative to the rate of carboxylation.

Effects of C_a on the rate of photosynthetic induction have been explored experimentally before (Chazdon and Pearcy, 1986; Naumburg and Ellsworth, 2000; Naumburg *et al*., 2001; Leakey *et al*., 2002; Tomimatsu and Tang, 2012; Tomimatsu *et al*., 2014; Soleh *et al*., 2016), and have been reviewed twice

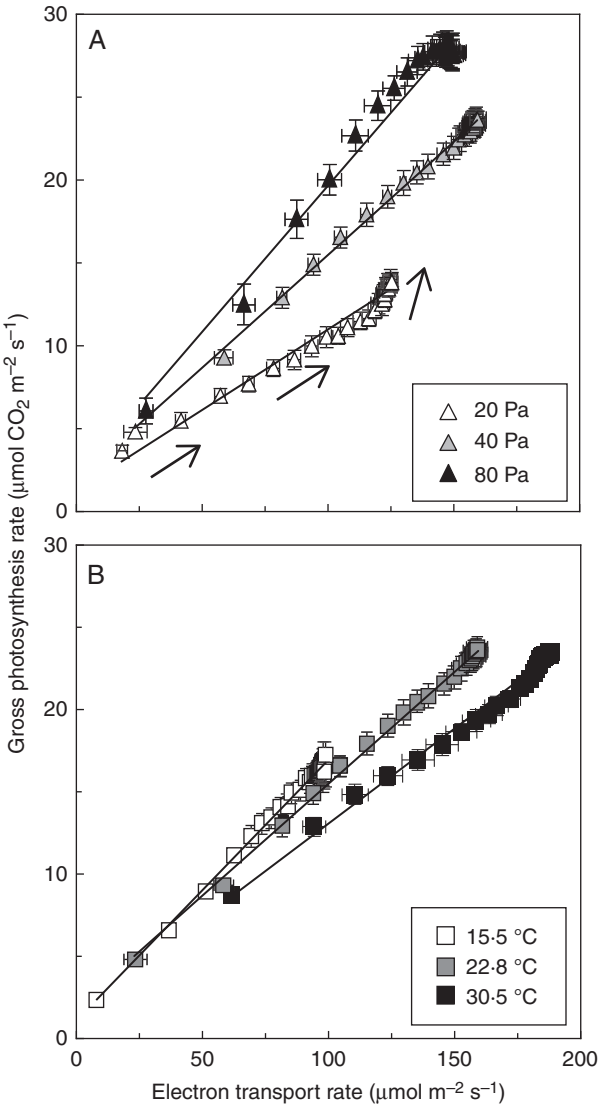

FIG. 7. Relationship between electron transport rate and gross photosynthesis rate ($A_n + R_d$) during photosynthetic induction, as affected by C_a (A) and T_{leaf} (B). Arrows indicate the direction of change over time. Mean ± SE ($n = 5$).

recently (Kaiser *et al.*, 2015; Tomimatsu and Tang, 2016). Kaiser *et al.* (2015) found that across studies, t_{A90} decreased near-linearly with increases in C_a, while t_{A50} was unaffected. In the current study, t_{A50} was significantly increased in low C_a, while t_{A90} was three times lower in high (6·2 min) compared to low C_a (18·5 min; Table 2). Altogether, the stronger response to C_a observed in the current study (compared to the general response summarized by Kaiser *et al.*, 2015) may be due to the use of C_3 plants with high photosynthetic rate compared to most species summarized by Kaiser *et al.* (2015).

Leaf temperature: effects on the rate of RuBP regeneration and on stomatal opening

Effects of different leaf temperatures on the rate of photosynthetic induction were small compared to those of C_a and $VPD_{leaf\text{-}air}$ (Fig. 1C), but they strongly affected the levels and kinetics of Φ_{PSII} and NPQ (Fig. 6B, D; discussed below). While apparent Rubisco activation rates were not significantly increased by elevated T_{leaf} (Fig. 4B), IS_{60} was significantly larger and t_{A50} significantly smaller (Table 2), suggesting a faster activation of the enzymes controlling the rate of RuBP regeneration (Sassenrath-Cole and Pearcy, 1992). This had slight effects on the initial relaxation of biochemical limitation (Fig. 3D). Stomatal opening was depressed at both low and high T_{leaf} (by 41–44 % compared to intermediate T_{leaf}): the difference between initial and final g_s was only 0·17 (low T_{leaf}) and 0·16 (high T_{leaf}), compared to 0·29 mol m^{-2} s^{-1} at intermediate T_{leaf} (Table 2). At the same time, the difference between initial and final A was virtually the same at intermediate and high T_{leaf}, while it was 30 % lower at low T_{leaf} (Table 2). Thus, while at low T_{leaf} (weak g_s and A increase) and intermediate T_{leaf} (strong g_s and A increase) diffusional limitation was low and comparable, at high T_{leaf} (combination of weak g_s increase and strong A increase) there was large diffusional limitation (Fig. 3C). The value of $VPD_{leaf\text{-}air}$ was only 0·04 kPa larger at high compared to intermediate T_{leaf} (File S2), and was therefore not responsible for the increase in diffusional limitation at high T_{leaf}.

The effect of T_{leaf} on the rate of photosynthetic induction has been explored several times in a spectrum of species and growth conditions (Küppers and Schneider, 1993; Pepin and Livingston, 1997; Leakey *et al.*, 2003; Yamori *et al.*, 2012; Carmo-Silva and Salvucci, 2013). Across these studies, increasing T_{leaf} decreased t_{A50} and t_{A90} up to an optimum of ~30 °C (i.e. smallest t_{A50} and t_{A90}, meaning highest rate of induction), above which these indices increased again (Kaiser *et al.*, 2015). Further, it was noted that effects of T_{leaf} on induction rates were not uniform between studies (Kaiser *et al.*, 2015). The data in the current study add to the scatter: t_{A50} was lower at high T_{leaf}, but t_{A90} was unaffected by treatment levels (Table 2). Apparently, there is large interspecific variation in the temperature response of photosynthetic induction.

$VPD_{leaf\text{-}air}$: lower g_s affects apparent Rubisco activation kinetics, diffusional limitation and WUE_i

Increases in $VPD_{leaf\text{-}air}$ (i.e. dryer air) strongly decreased g_s before, during and after photosynthetic induction (Fig. 1F). Very high $VPD_{leaf\text{-}air}$ even induced stomatal oscillations (feeding back on A), a phenomenon whose mechanisms are still under debate (Buckley, 2005; Kaiser, 2009; Kaiser and Paoletti, 2014). By decreasing C_c (File S6), elevated $VPD_{leaf\text{-}air}$ slowed down the rate of photosynthetic induction (Fig. 1E). This had strong effects on diffusional and, surprisingly, biochemical limitations (Fig. 3E, F), by decreasing the rate of apparent Rubisco activation (Fig 4B). A $VPD_{leaf\text{-}air}$ effect on apparent Rubisco activation rates has, to our knowledge, not been found before. Slower apparent Rubisco activation is probably caused by lower C_i or C_c during induction, as indicated by the relationships of τ_R with the relative rate of C_i decrease and the lowest partial pressure of C_c reached during induction (Fig. 5). Further support for this hypothesis comes from a study on water stress: short-term leaf desiccation, which led to stomatal closure, decreased both C_c and initial (i.e. extracted) Rubisco activity (Flexas *et al.*, 2006). While the rate of Rubisco activation after

a dark–light transition and initial Rubisco activity are not the same, they are both likely to be affected by the rate or the total extent of carbamylation, respectively. Furthermore, apparent Rubisco activation rates after increases in irradiance correlated positively with C_i (see above).

While higher $VPD_{leaf\text{-}air}$ undoubtedly had a negative impact on A after illumination was raised, it had positive effects on WUE_i (Fig. 2C). The global climate is predicted to be dryer (at least in mid-latitude and subtropical regions), warmer and enriched in CO_2 (IPCC, 2013). It can thus be hypothesized that WUE_i in such a climate will increase in fluctuating irradiance, as increases in all of these factors improved WUE_i (Fig. 2).

In contrast to C_a and T_{leaf}, published data describing the effects of $VPD_{leaf\text{-}air}$ on rates of photosynthetic induction are scarce. Nevertheless, Tinoco-Ojanguren and Pearcy (1993*a*, *b*) reported that high VPD decreased steady-state g_s, slowed down photosynthetic induction and increased stomatal limitations in a pioneer rainforest tree (*Piper auritum*) and a shade-tolerant shrub (*Piper aequale*), similar to the present findings on tomato. Thus, stomatal dynamics of widely varying species seem to be similarly affected by elevated $VPD_{leaf\text{-}air}$.

Lack of effects of blue irradiance: possible reasons

Surprisingly, varying blue irradiance (0–20 %) had no effects on stomatal opening or photosynthetic induction (Table 2). Blue irradiance generally promotes rapid stomatal opening when combined with red irradiance, and could be a cue for overall radiation load (Shimazaki *et al*., 2007). In the current experiment, 1000 µmol m^{-2} s^{-1} may have provided such a strong stimulus for stomatal opening that the rate of opening could not have been accelerated by increasing the percentage of blue irradiance. Assmann and Grantz (1990*a*, *b*), however, superimposed blue irradiance on 900 µmol m^{-2} s^{-1} red irradiance in sugarcane and soybean and found an additional opening response (data on photosynthesis were not shown in these studies). The reported effects of blue irradiance on photosynthetic induction are ambiguous: Košvancová-Zitová *et al*. (2009) reported faster induction in beech (*Fagus sylvatica* L.) with increasing blue irradiance (25–75 % blue irradiance in 800 µmol m^{-2} s^{-1}), while data reported in Zhang *et al*. (2011) for the orchid *Cypripedium flavum* showed the opposite (0–100 % blue irradiance in 250 µmol m^{-2} s^{-1}). The effects of blue irradiance on induction are therefore variable with no clear correlations between the effects of blue irradiance and other environmental responses or preferences.

Changes in chlorophyll fluorescence parameters during photosynthetic induction

Changes in Φ_{PSII} during induction were primarily explained by changes in photochemical quenching (q_P) rather than F_v'/F_m'. Overall, this suggests that changes in NPQ, acting via decreases in F_v'/F_m', did not contribute substantially to the changes in Φ_{PSII} (Baker *et al*., 2007); the total span of changes of F_v'/F_m' was 0·55–0·65, while that for q_P was 0·05–0·7 (File S7). Changes in q_P occurred in the first 12 min of induction, making its time course similar to that of Φ_{PSII}, but distinct from that of NPQ (Fig. 6). Steady-state Φ_{PSII} was slightly higher in ambient compared to high C_a (Fig. 6A), while NPQ was slightly higher in high compared to ambient C_a (Fig. 6C). This may be explained by triose phosphate utilization limitation slowing down ETR in high C_a.

All C_a and T_{leaf} treatments (except low T_{leaf}) produced initial overshoots in NPQ (Fig. 6). It is hypothesized that the overshoot was caused by low metabolic activity that resulted in a low rate of electron transport, which caused a decrease in lumen pH, thereby activating NPQ. Upon the subsequent activation of Calvin cycle enzymes and increase in linear electron transport, the lumen pH increased and energy-dependent quenching (q_E) decreased, lowering NPQ. The slow build-up of zeaxanthin during induction would then have produced a slower increase in energy-dependent quenching (q_E) by enhancing the effect of pH on NPQ. This was visible between minutes 20 and 60 in all treatments except high T_{leaf} (Bilger and Björkman, 1991). Leaves that contained fully activated Rubisco in low irradiance did not exhibit an NPQ overshoot when transferred to high irradiance (Carmo-Silva and Salvucci, 2013). Also, in leaves containing less Rubisco activase, NPQ kept increasing throughout induction, indicating that Rubisco activation, and by implication photochemical quenching, increased more slowly (Yamori *et al*., 2012). Both examples demonstrate how the rate of change of metabolism sets the demand for the products of electron transport during photosynthetic induction, thereby affecting the transient excess irradiance condition and the parallel induction of NPQ.

Mesophyll conductance

The change in g_m during photosynthetic induction has, to our knowledge, never been assessed. This has been attempted here using the often-used variable J method (Harley *et al*., 1992) (File S5). However, because possible changes in alternative electron transport, stoichiometry of ATP and NADPH production, leaf absorbance (due to chloroplast movement), R_d, and the overall validity of g_m especially in the early phases of induction cannot be accounted for, we refrain from speculations on the correctness of g_m during photosynthetic induction, but note this as a topic that deserves more dedicated experimentation. Two more things are noteworthy: firstly, the steady-state values of g_m (Table in File S5) compare very well to published data (Bernacchi *et al*., 2002; Flexas *et al*., 2008; von Caemmerer and Evans, 2015). Secondly, the fact that at the beginning of photosynthetic induction none of the slopes of A_{gr}/ETR (Fig. 7) deviated strongly from linearity implies that neither changes in g_s nor changes in g_m limited induction, as in such a case C_c would have dropped momentarily (oxygenation would have increased relative to carboxylation). This suggests that potentially low g_m was not a (strongly) limiting factor during photosynthetic induction.

Methodological considerations

Diffusional and biochemical limitation were calculated for the first time assuming a curvilinear A/C_i relationship instead of the linear relationship previously used in such analyses (e.g. Woodrow and Mott, 1989; Jackson *et al*., 1991; Allen and

TABLE 3. *Change (%) in net photosynthesis rate or intrinsic water use efficiency (WUE_i) if either Rubisco activated directly after illumination or stomatal conductance directly increased to its final, steady-state value*

Treatment	Net photosynthesis rate		WUE_i	
	Rubisco kinetics	Stomatal opening	Rubisco kinetics	Stomatal opening
20 Pa	7·5±1·5	3·6±0·8	24·7±1·7	−32·1±2·0
40 Pa	5·6±0·4	1·1±0·1	12·2±0·9	−20·6±1·4
80 Pa	2·5±0·6	0·6±0·1	5·8±0·8	−19·8±2·2
15·5 °C	5·2±0·7	1·4±0·3	11·7±1·8	−24·7±6·3
22·8 °C	5·6±0·4	1·1±0·1	12·2±0·9	−20·6±1·4
30·5 °C	4·1±0·9	3·3±1·2	11·5±1·3	−13·9±2·6
0·5 kPa	4·9±0·4	1·4±0·4	11·5±1·3	−23·3±3·6
0·8 kPa	5·6±0·4	1·1±0·1	12·2±0·9	−20·6±1·4
1·6 kPa	7·6±0·6	0·6±0·2	18·5±2·2	−15·6±2·5
2·3 kPa	8·0±0·8	0·7±0·1	17·3±2·1	−13·7±2·1

Values are means over minutes 2–60 during photosynthetic induction ± SE ($n = 5$).

Pearcy, 2000). This strongly affected the estimation of diffusional limitation at 40 and 80 Pa (Supplementary Data File S8). Most studies using this correction were performed with atmospheric or below-atmospheric C_a, where assuming a linear A/C_i relationship may be reasonable. However, some authors used a linear relationship at C_a of ≥ 70 Pa (Košvancová-Zitová *et al*., 2009; Tomimatsu and Tang, 2012). Their measures of stomatal limitation in high C_a are probably substantial overestimations.

In light-adapted leaves, the conventionally measured F_m' (obtained using single saturating pulses) underestimated 'true' F_m' (obtained using multiple saturating pulses), by approx. 4 %. It is shown here for the first time that this underestimation develops within 10 min during induction (File S3). Steady-state measurements on tobacco, pea and maize leaves (grown at 300 µmol m^{-2} s^{-1}) showed comparably large underestimations of F_m', translating into underestimations of Φ_{PSII} (Loriaux *et al*., 2013). Here, steady-state Φ_{PSII} would have been underestimated by 8–15 % if single rather than multi-phase pulses were used.

Improving crop photosynthesis in fluctuating irradiance: why and how?

Improving crop productivity via photosynthetic efficiency is considered a crucial pathway for future global food security (Zhu *et al*., 2010). Faster regulation of Rubisco activity may increase A in naturally fluctuating irradiance (Carmo-Silva *et al*., 2015). Also, a more dynamically regulated g_s, which can, for example, be reached by smaller stomata, could help save water by increasing dynamic WUE_i (Drake *et al*., 2013; Lawson and Blatt, 2014). Two scenarios were therefore explored using the present data on induction rates and stomatal opening in various atmospheres: changes in average A and WUE_i during photosynthetic induction in the case of (1) instantaneous Rubisco activation and (2) instantaneous g_s increase.

The analysis (Table 3) revealed that average A could increase by 6–8 % in ambient C_a (across $VPD_{leaf\text{-}air}$ and T_{leaf} treatments), if Rubisco activated instantaneously. In elevated C_a, a form of Rubisco that activates instantaneously would be less advantageous (2·5 instead of 5·6 % increase in A), because Rubisco already activates faster in high C_a. The faster increase in A due to faster Rubisco activation would also positively impact WUE_i, by up to 12–19 % in ambient C_a. Rubisco activation can be sped up by manipulating the isoform composition of Rubisco activase (Zhang *et al*., 2002), although always-active Rubisco activase reduced growth in the *Arabidopsis thaliana* mutant *rwt43* compared to its wild type (Carmo-Silva and Salvucci, 2013). The elucidation of how the activation state of Rubisco affects the balance of intermediates in the Calvin cycle should therefore be central to future research on improving dynamic photosynthesis.

Instantaneous stomatal opening would improve average photosynthesis rates by up to 1–3 % in ambient C_a and across air humidities and leaf temperatures. Thus, increasing the kinetics of Rubisco activation seems to be a more useful strategy than increasing g_s, especially as higher g_s would strongly decrease WUE_i (by 21–25 % in ambient C_a). Stomata that react faster to decreases in irradiance, on the other hand, would be very beneficial for dynamic WUE_i (Lawson and Blatt 2014); whether or not quickly reacting stomata enhance WUE_i is therefore dependent on the situation.

A transition from completely inactivated photosynthesis in darkness to near-saturating irradiance does not represent natural conditions; the modulation of dynamic photosynthesis by environmental factors and the benefits of faster Rubisco activation or stomatal opening may be smaller when photosynthesis is somewhat induced. Therefore, these numbers can only be used to provide a first guess for the benefits of 'immediate' Rubisco activation or stomatal opening.

CONCLUSIONS

Increased CO_2 partial pressure led to faster photosynthetic induction, by decreasing diffusional limitation and by speeding up the relaxation of biochemical limitation. Increased leaf temperature led to slightly faster induction rates, due to faster relaxation of biochemical limitation. Elevated leaf-to-air vapour pressure deficit mainly lowered the relaxation rates of biochemical limitation, by slowing down apparent Rubisco activation via decreased availability of CO_2. Increasing the rates of Rubisco activation would be more beneficial for dynamic photosynthesis than increasing initial stomatal conductance or the rate of stomatal opening.

SUPPLEMENTARY DATA

Supplementary data are available online at www.aob.oxfordjournals.org and consist of the following. File S1: preliminary irradiance response curves. File S2: traces of $VPD_{leaf\text{-}air}$ during photosynthetic induction as affected by T_{leaf}. File S3: measured F_m' underestimates true F_m' in light-adapted but not in dark-adapted leaves. File S4: A/C_i and A/PAR curves. File S5: changes in g_m during photosynthetic induction. File S6: changes of chloroplast CO_2 partial pressure (C_c) during photosynthetic induction. File S7: q_P and F_v'/F_m' during photosynthetic induction. File S8: implications of using curvilinear instead of linear A/C_c relationships when determining diffusional limitation.

ACKNOWLEDGEMENTS

We thank Shizue Matsubara, Tracy Lawson, Tsu-Wei Chen and Alejandro Morales for useful discussions. This work was supported by the BioSolar Cells open innovation consortium, supported by the Dutch Ministry of Economic Affairs, and by Powerhouse.

LITERATURE CITED

Allen MT, Pearcy RW. 2000. Stomatal versus biochemical limitations to dynamic photosynthetic performance in four tropical rainforest shrub species. *Oecologia* **122**: 479–486.

Assmann SM, Grantz DA. 1990*a*. Stomatal response to humidity in sugarcane and soybean: effect of vapour pressure difference on the kinetics of the blue light response. *Plant, Cell & Environment* **13**: 163–169.

Assmann SM, Grantz DA. 1990*b*. The magnitude of the stomatal response to blue light: modulation by atmospheric humidity. *Plant Physiology* **93**: 701–709.

Baker NR, Harbinson J, Kramer DM. 2007. Determining the limitations and regulation of photosynthetic energy transduction in leaves. *Plant, Cell & Environment* **30**: 1107–1125.

Bernacchi CJ, Portis AR, Nakano H, von Caemmerer S, Long SP. 2002. Temperature response of mesophyll conductance. Implications for the determination of Rubisco enzyme kinetics and for limitations to photosynthesis in vivo. *Plant Physiology* **130**: 1992–1998.

Bernacchi CJ, Singsaas EL, Pimentel C, Portis AR, Long SP. 2001. Improved temperature response functions for models of Rubisco-limited photosynthesis. *Plant, Cell & Environment* **24**: 253–259.

Bilger W, Björkman O. 1991. Temperature dependence of violaxanthin deepoxidation and non-photochemical fluorescence quenching in intact leaves of *Gossypium hirsutum* L. and *Malva parviflora* L. *Planta* **184**: 226–234.

Buckley TN. 2005. The control of stomata by water balance. *New Phytologist* **168**: 275–292.

von Caemmerer S, Evans JR. 2015. Temperature responses of mesophyll conductance differ greatly between species. *Plant, Cell & Environment* **38**: 629–637.

Carmo-Silva AE, Salvucci ME. 2013. The regulatory properties of Rubisco activase differ among species and affect photosynthetic induction during light transitions. *Plant Physiology* **161**: 1645–1655.

Carmo-Silva AE, Scales JC, Madgwick PJ, Parry MAJ. 2015. Optimizing Rubisco and its regulation for greater resource use efficiency. *Plant, Cell & Environment* **38**: 1817–1832.

Chazdon RL, Pearcy RW. 1986. Photosynthetic responses to light variation in rainforest species I. Induction under constant and fluctuating light conditions. *Oecologia* **69**: 517–523.

Drake PL, Froend RH, Franks PJ. 2013. Smaller, faster stomata: scaling of stomatal size, rate of response, and stomatal conductance. *Journal of Experimental Botany* **64**: 495–505.

Farquhar GD, von Caemmerer S, Berry JA. 1980. A biochemical model of photosynthetic CO_2 assimilation in leaves of C_3 species. *Planta* **149**: 78–90.

Flexas J, Diaz-Espejo A, Galmés J, Kaldenhoff R, Medrano H, Ribas-Carbo M. 2007. Rapid variations of mesophyll conductance in response to changes in CO_2 concentration around leaves. *Plant, Cell & Environment* **30**: 1284–1298.

Flexas J, Ribas-Carbó M, Bota J, *et al.* 2006. Decreased Rubisco activity during water stress is not induced by decreased relative water content but related to conditions of low stomatal conductance and chloroplast CO_2 concentration. *The New Phytologist* **172**: 73–82.

Flexas J, Ribas-Carbó M, Diaz-Espejo A, Galmés J, Medrano H. 2008. Mesophyll conductance to CO_2: current knowledge and future prospects. *Plant, Cell & Environment* **31**: 602–621.

Genty B, Briantais JM, Baker NR. 1989. The relationship between the quantum yield of photosynthetic electron transport and quenching of chlorophyll fluorescence. *Biochimica et Biophysica Acta* **990**: 87–92.

Harley PC, Loreto F, Di Marco G, Sharkey TD. 1992. Theoretical considerations when estimating the mesophyll conductance to CO_2 flux by analysis of the response of photosynthesis to CO_2. *Plant Physiology* **98**: 1429–1436.

IPCC. 2013. *Fifth assessment report climate change 2013: summary for policymakers*. Cambridge: Cambridge University Press.

Jackson RB, Woodrow IE, Mott KA. 1991. Nonsteady-state photosynthesis following an increase in photon flux density (PFD): effects of magnitude and duration of initial PFD. *Plant Physiology* **95**: 498–503.

Johnson GN, Young AJ, Horton P. 1994. Activation of non-photochemical quenching in thylakoids and leaves. *Planta* **194**: 550–556.

Kaiser H. 2009. The relation between stomatal aperture and gas exchange under consideration of pore geometry and diffusional resistance in the mesophyll. *Plant, Cell & Environment* **32**: 1091–1098.

Kaiser E, Morales A, Harbinson J, Heuvelink E, Prinzenberg AE, Marcelis LFM. 2016. Metabolic and diffusional limitations of photosynthesis in fluctuating irradiance in *Arabidopsis thaliana*. *Scientific Reports* doi:10.1038/sr.

Kaiser E, Morales A, Harbinson J, Kromdijk J, Heuvelink E, Marcelis LFM. 2015. Dynamic photosynthesis in different environmental conditions. *Journal of Experimental Botany* **66**: 2415–2426.

Kaiser H, Paoletti E. 2014. Dynamic stomatal changes. In: M Tausz, N Grulke, eds. *Plant ecophysiology. Trees in a changing environment*. Dordrecht: Springer Netherlands, 61–82.

Košvancová M, Urban O, Šprtová M, *et al.* 2009. Photosynthetic induction in broadleaved *Fagus sylvatica* and coniferous *Picea abies* cultivated under ambient and elevated CO_2 concentrations. *Plant Science* **177**: 123–130.

Košvancová-Zitová M, Urban O, Navrátil M, Špunda V, Robson TM, Marek M V. 2009. Blue radiation stimulates photosynthetic induction in *Fagus sylvatica* L. *Photosynthetica* **47**: 388–398.

Küppers M, Schneider H. 1993. Leaf gas exchange of beech (*Fagus sylvatica* L.) seedlings in lightflecks: effects of fleck length and leaf temperature in leaves grown in deep and partial shade. *Trees* **7**: 160–168.

Lawson T, Blatt MR. 2014. Stomatal size, speed, and responsiveness impact on photosynthesis and water use efficiency. *Plant Physiology* **164**: 1556–1570.

Leakey ADB, Press MC, Scholes JD. 2003. High-temperature inhibition of photosynthesis is greater under sunflecks than uniform irradiance in a tropical rain forest tree seedling. *Plant, Cell & Environment* **26**: 1681–1690.

Leakey ADB, Press MC, Scholes JD, Watling JR. 2002. Relative enhancement of photosynthesis and growth at elevated CO_2 is greater under sunflecks than uniform irradiance in a tropical rain forest tree seedling. *Plant, Cell and Environment* **25**: 1701–1714.

Long SP, Bernacchi CJ. 2003. Gas exchange measurements, what can they tell us about the underlying limitations to photosynthesis? Procedures and sources of error. *Journal of Experimental Botany* **54**: 2393–2401.

Loriaux SD, Avenson TJ, Welles JM, *et al.* 2013. Closing in on maximum yield of chlorophyll fluorescence using a single multiphase flash of sub-saturating intensity. *Plant, Cell & Environment* **36**: 1755–1570.

Mott KA, Woodrow IE. 1993. Effects of O_2 and CO_2 on nonsteady-state photosynthesis. Further evidence for ribulose-1,5-bisphosphate carboxylase/oxygenase limitation. *Plant Physiology* **102**: 859–866.

Murchie EH, Niyogi KK. 2011. Manipulation of photoprotection to improve plant photosynthesis. *Plant Physiology* **155**: 86–92.

Naumburg E, Ellsworth DS. 2000. Photosynthetic sunfleck utilization potential of understory saplings growing under elevated CO_2 in FACE. *Oecologia* **122**: 163–174.

Naumburg E, Ellsworth DS, Katul GG. 2001. Modeling dynamic understory photosynthesis of contrasting species in ambient and elevated carbon dioxide. *Oecologia* **126**: 487–499.

Osterhout WJ V, Haas ARC. 1918. Dynamical aspects of photosynthesis. *Proceedings of the National Academy of Sciences, USA* **4**: 85–91.

Oxborough K, Baker NR. 1997. Resolving chlorophyll a fluorescence images of photosynthetic efficiency into photochemical and non-photochemical components – calculation of qP and F_v'/F_m' without measuring F_o'. *Photosynthesis Research* **54**: 135–142.

Pearcy RW, Krall JP, Sassenrath-Cole GF. 1996. Photosynthesis in fluctuating light environments. In: Baker NR, ed. *Photosynthesis and the Environment*. Dordrecht: Kluwer, 321–346.

Pearcy RW, Way DA. 2012. Two decades of sunfleck research: looking back to move forward. *Tree Physiology* **32**: 1059–1061.

Pepin S, Livingston NJ. 1997. Rates of stomatal opening in conifer seedlings in relation to air temperature and daily carbon gain. *Plant, Cell & Environment* **20**: 1462–1472.

Pons TL, Welschen RAM. 2002. Overestimation of respiration rates in commercially available clamp-on leaf chambers. Complications with measurement of net photosynthesis. *Plant, Cell & Environment* **25**: 1367–1372.

Sassenrath-Cole GF, Pearcy RW. 1992. The role of ribulose-1,5-bisphosphate regeneration in the induction requirement of photosynthetic CO_2 exchange under transient light conditions. *Plant Physiology* **99**: 227–234.

Sharkey TD. 1985. O_2-insensitive photosynthesis in C_3 plants. Its occurrence and a possible explanation. *Plant Physiology* **78**: 71–75.

Sharkey TD, Bernacchi CJ, Farquhar GD, Singsaas EL. 2007. Fitting photosynthetic carbon dioxide response curves for C_3 leaves. *Plant, Cell and Environment* **30**: 1035–1040.

Shimazaki K, Doi M, Assmann SM, Kinoshita T. 2007. Light regulation of stomatal movement. *Annual Review of Plant Biology* **58**: 219–247.

Soleh MA, Tanaka Y, Nomoto Y, *et al.* 2016. Factors underlying genotypic differences in the induction of photosynthesis in soybean [*Glycine max* (L.) Merr.]. *Plant, Cell & Environment* **39**: 685–693.

Tinoco-Ojanguren C, Pearcy RW. 1993. Stomatal dynamics and its importance to carbon gain in two rainforest Piper species. II. Stomatal versus biochemical limitations during photosynthetic induction. *Oecologia* **94**: 395–402.

Tomimatsu H, Iio A, Adachi M, Saw L-G, Fletcher C, Tang Y. 2014. High CO_2 concentration increases relative leaf carbon gain under dynamic light in *Dipterocarpus sublamellatus* seedlings in a tropical rain forest, Malaysia. *Tree Physiology* **34**: 944–954.

Tomimatsu H, Tang Y. 2012. Elevated CO_2 differentially affects photosynthetic induction response in two Populus species with different stomatal behavior. *Oecologia* **169**: 869–878.

Tomimatsu H, Tang Y. 2016. Effects of high CO_2 levels on dynamic photosynthesis: carbon gain, mechanisms, and environmental interactions. *Journal of Plant Research* **129**: 365–377.

Urban O, Košvancová M, Marek M V, Lichtenthaler HK. 2007. Induction of photosynthesis and importance of limitations during the induction phase in sun and shade leaves of five ecologically contrasting tree species from the temperate zone. *Tree Physiology* **27**: 1207–1215.

Woodrow IE, Kelly ME, Mott KA. 1996. Limitation of the rate of ribulosebisphosphate carboxylase activation by carbamylation and ribulosebisphosphate carboxylase activase activity: development and tests of a mechanistic model. *Australian Journal of Plant Physiology* **23**: 141–149.

Woodrow IE, Mott KA. 1989. Rate limitation of non-steady-state photosynthesis by ribulose-1,5-bisphosphate carboxylase in spinach. *Australian Journal of Plant Physiology* **16**: 487–500.

Yamori W, Masumoto C, Fukayama H, Makino A. 2012. Rubisco activase is a key regulator of non-steady-state photosynthesis at any leaf temperature and, to a lesser extent, of steady-state photosynthesis at high temperature. *The Plant Journal* **71**: 871–880.

Yin X, Struik PC, Romero P, *et al.* 2009. Using combined measurements of gas exchange and chlorophyll fluorescence to estimate parameters of a biochemical C_3 photosynthesis model: a critical appraisal and a new integrated approach applied to leaves in a wheat (*Triticum aestivum*) canopy. *Plant, Cell & Environment* **32**: 448–464.

Zhang SB, Guan ZJ, Chang W, Hu H, Yin Q, Cao KF. 2011. Slow photosynthetic induction and low photosynthesis in *Paphiopedilum armeniacum* are related to its lack of guard cell chloroplast and peculiar stomatal anatomy. *Physiologia Plantarum* **142**: 118–127.

Zhang N, Kallis RP, Ewy RG, Portis AR. 2002. Light modulation of Rubisco in *Arabidopsis* requires a capacity for redox regulation of the larger Rubisco activase isoform. *Proceedings of the National Academy of Sciences, USA* **99**: 3330–3334.

Zhu XG, Long SP, Ort DR. 2010. Improving photosynthetic efficiency for greater yield. *Annual Review of Plant Biology* **61**: 235–261.